



Available online at www.sciencedirect.com

ScienceDirect

Geochimica et Cosmochimica Acta 304 (2021) 178-190

Geochimica et Cosmochimica Acta

www.elsevier.com/locate/gca

Spatial characteristics and removal of dissolved black carbon in the western Arctic Ocean and Bering Sea

Ziming Fang a,b, Weifeng Yang a,*, Aron Stubbins c,*, Min Chen a, Junjie Li a, Renming Jia a, Qi Li a, Jing Zhu a, Bo Wang a

^a State Key Laboratory of Marine Environmental Science and College of Ocean and Earth Sciences, Xiamen University, Xiamen 361102, China
 ^b Department of Ocean Science, The Hong Kong University of Science and Technology, Clear Water Bay, Kowloon, Hong Kong
 ^c Departments of Marine and Environmental Sciences, Civil and Environmental Engineering, and Chemistry and Chemical Biology,
 Northeastern University, Boston, MA 02115, USA

Received 24 July 2020; accepted in revised form 17 April 2021; available online 27 April 2021

Abstract

In the Arctic, large amounts of black carbon (BC) are released into river water and transported to the oceans as dissolved BC (DBC). However, the cycling and fate of DBC in the ocean is poorly understood. Here, DBC, dissolved organic carbon (DOC), absorbance, and δ^{18} O were analyzed to examine the spatial characteristics and removal of DBC in the western Arctic Ocean and the Bering Sea during the boreal summer. DBC concentrations ranged from 0.67 to 4.18 µmol-C L⁻¹. In the sea-ice free regions, high DBC and DOC concentrations and a254 values corresponded to high δ^{18} O-derived meteoric water contents, indicating that river discharge dominated their spatial patterns. By contrast, sea-ice meltwater (SIM) appeared to dilute DBC and DOC in SIM impacted waters (SIM > 3.5%). The departure of DBC from conservative mixing lines suggested that 47–84% of riverine DBC was removed over the shelves with 7–23% transported to the upper Canada Basin. These results suggest that shelf regions are crucial sites for riverine DBC removal that modulate the delivery of DBC to the open Arctic Ocean. © 2021 Elsevier Ltd. All rights reserved.

Keywords: Dissolved black carbon; Dissolved organic carbon; Bering Sea; Arctic Ocean; Chukchi Sea

1. INTRODUCTION

Black carbon (BC) is derived from incomplete combustion of biomass and fossil fuel (Goldberg, 1985). Biomass burning (including natural and anthropogenic) generates 40–215 Tg-C yr $^{-1}$ of BC, of which $34 \pm 26\%$ is exported to the oceans via river discharge, making the ocean the major sink of BC (Jaffé et al., 2013; Jones et al., 2020). Dissolved BC (DBC), the largest pool of molecularly identifiable DOC in the aquatic environment (Dittmar and Stubbins, 2014), accounts for about 2% of global marine

DOC (~14 Tg) (Dittmar and Paeng, 2009). Yet, the fate and cycling of DBC in the oceans remains enigmatic. The 14 C-age of DBC in surface waters is thousands of years younger than that in the deep ocean (Ziolkowski and Druffel, 2010; Coppola and Druffel, 2016), indicating that DBC persists in the deep, dark ocean for a long time. However, the riverine DBC discharge of 18 ± 4 Tg yr $^{-1}$ (Jones et al., 2020) is sufficient to replace the global oceanic pool of DBC within several hundreds of years (Wagner et al., 2018). Despite this apparent oversupply of riverine DBC to the oceans, the δ^{13} C signature of Atlantic and Pacific Ocean DBC is distinct from that of riverine DBC, indicating the DBC in the oceans is marigenous not terrigenous (Wagner et al., 2019). Thus, there must be efficient removal pathways for riverine DBC before it reaches the deep

northeastern.edu (A. Stubbins).

^{*} Corresponding authors.

E-mail addresses: wyang@xmu.edu.cn (W. Yang), a.stubbins@

ocean. Losses of DBC at sea could be caused by photochemical removal (Stubbins et al., 2012a) or sorption to sinking particles (Coppola et al., 2014; Fang et al., 2016). However, where and how DBC is removed during transport from the river to the open ocean remain questions for understanding the fate of DBC at sea. Removal of terrigenous dissolved organic carbon (DOC) can occur as riverderived DOC transits the continental shelves to the open ocean (Letscher et al., 2011). Thus, we hypothesize that shelves are also sites of riverine DBC loss.

The Arctic Ocean receives more than 10% of the global riverine DOC, but holds just 1% of the global ocean volume (Opsahl et al., 1999). Arctic rivers have higher DBC content than temperate rivers (Jones et al., 2020). Annually, about 2.8 Tg of DBC are delivered to the Arctic Ocean from the Pan-Arctic watershed, accounting for ~ 8% of the Arctic riverine DOC flux (Stubbins et al., 2015). In addition, atmospheric deposition of BC is also a potential DBC source to the Arctic Ocean (Khan et al., 2017; Mori et al., 2020). As a result, the Arctic Ocean receives the most intense DBC load among the oceans (Stubbins et al., 2015; Jones et al., 2020). Meanwhile, the Arctic Ocean has the widest shelf area. Thus, the Arctic Ocean is an important site for investigating the removal and fate of riverine DBC at sea. However, DBC cycling is poorly understood in the Arctic Ocean due to a paucity of data (Nakane et al., 2017).

To address this knowledge gap, seawater samples from the shelves and basins of the Bering Sea and western Arctic Ocean were analyzed for DBC, DOC and colored dissolved organic matter (CDOM). The stable oxygen isotopes of seawater (δ^{18} O) were also determined to estimate the fractions

of meteoric water (including river water and precipitation) and sea-ice meltwater (SIM) in samples. The objectives of this study were: (i) to examine the spatial patterns of DBC in the western Arctic Ocean and Bering Sea; (ii) to determine the roles of river discharge and sea-ice melting in regulating DBC distribution; and (iii) to evaluate the removal of riverine DBC in the Arctic Ocean.

2. MATERIALS AND METHODS

2.1. Study area

Sampling was conducted in the Bering Sea and western Arctic Ocean during the 7th Chinese Arctic Research Expedition (11 July to 26 September 2016). Major surface current systems and water masses in the study area are shown in Figs. 1 and S1. The Bering Slope Current flows northward along the Bering slope and divides the Bering Sea into basin and shelf (Coachman, 1986; Li et al., 2017). On the eastern Bering Shelf, the northward Pacific inflow can be separated into two branches, i.e., the Alaskan Coastal Water located to the east of 170.5°W (Figs. 2 and S1) as being confined by S < 31.8 (Coachman and Aagaard, 1974; Li et al., 2017) and the local Bering Shelf Water next to the Alaskan Coastal Water with salinity of 31.8-32.5 (Coachman et al., 1975; Coachman, 1986; Zhao et al., 2006). The hydrography of the Chukchi Sea during our sampling was characterized by steep gradients of salinity and temperature in surface water around 71°N (Figs. 3a and 3b). Surface water in the southern Chukchi Sea (<71° N) was saltier and warmer than in the northern Chukchi Sea (71–73°N) (Table 1 and Fig. 3). In the Canada Basin,

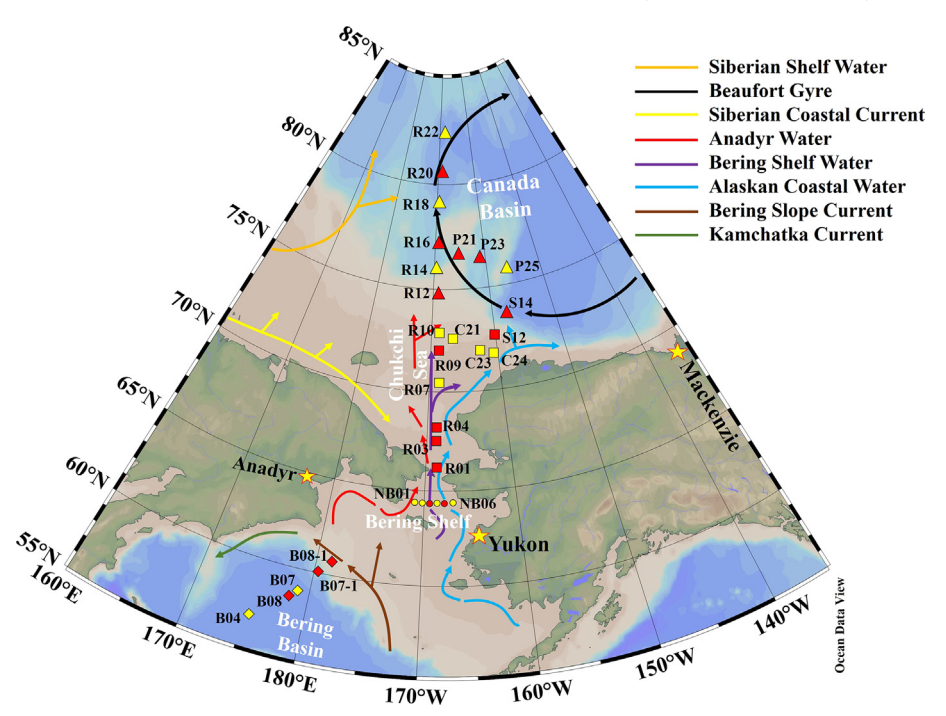


Fig. 1. Sampling stations and major currents in the western Arctic Ocean and Bering Sea (Modified from Li et al., 2017). DOC, CDOM and other basic parameters (i.e., δ^{18} O, temperature and salinity) are available for all stations (red and yellow), while DBC samples are only collected at selective stations (red). Stations in different regions are marked with different symbols, i.e., diamond: Bering Basin; circle: Bering Shelf, square: Chukchi Sea; Triangle: Canada Basin.

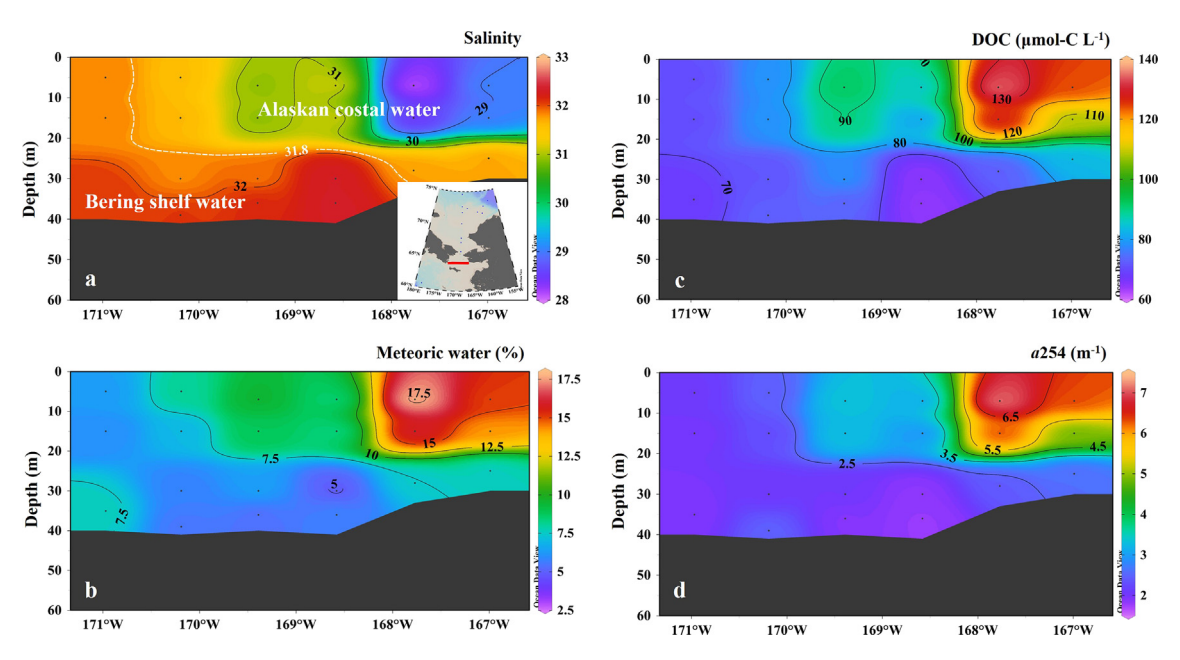


Fig. 2. Vertical distributions of salinity, meteoric water fraction, DOC and CDOM (i.e., a254) along the Bering Shelf section.

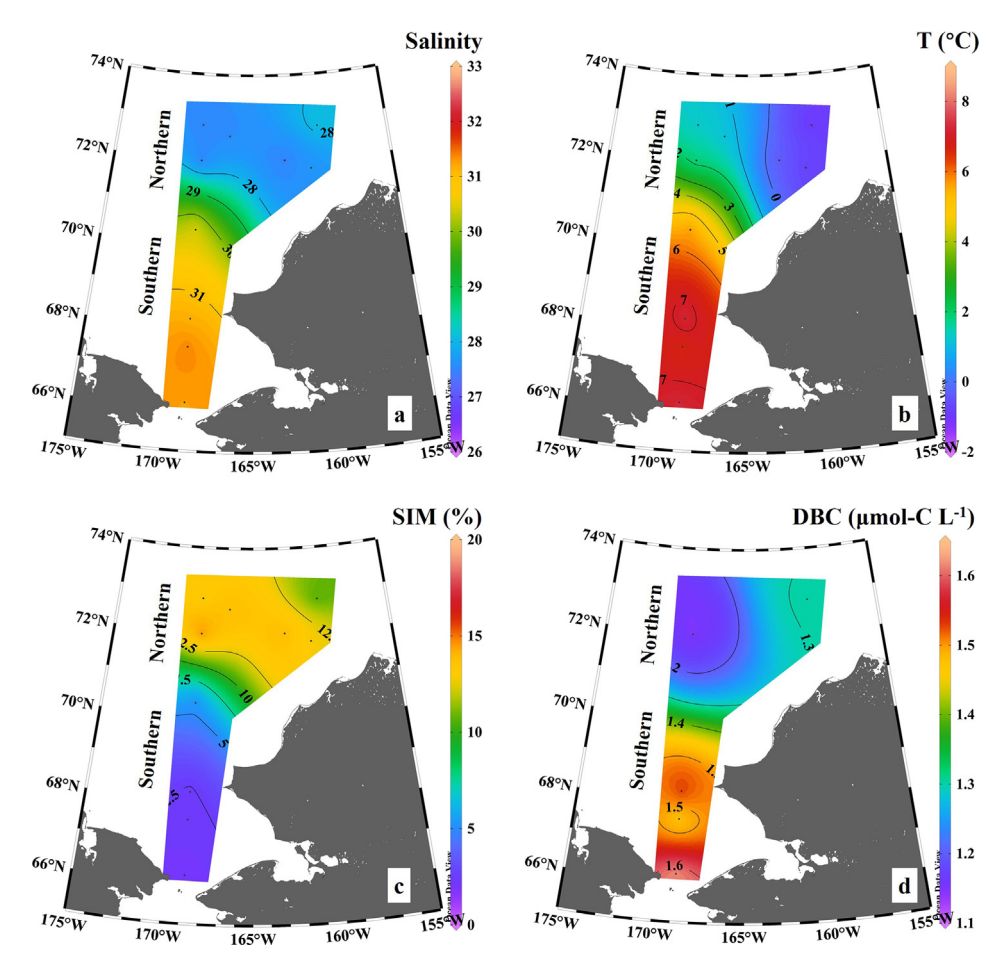


Fig. 3. Distributions of salinity, temperature, SIM fractions and DBC concentrations in the surface water of the Chukchi Sea.

Table 1 Physical and chemical parameters of various water masses in the western Arctic Ocean and Bering Sea.

Study region	Depth	S	T	SIM	Meteoric water	a254	DOC	SUVA ₂₅₄	n	DBC	B6/B5	DBC/ DOC	n
	(m)		(°C)	(%)	(%)	(m^{-1})	$\substack{(\mu mol\text{-}C\\L^{-1})}$	$\begin{array}{c} (L \ mg^{-1} \\ m^{-1}) \end{array}$		$\begin{array}{c} (\mu mol\text{-}C \\ L^{-1}) \end{array}$		(%)	
Bering Basin													
Surface water	0-50	32.73 ± 0.22	8.0 ± 3.1	1.3 ± 0.9	4.1 ± 0.6	1.7 ± 0.2	64 ± 5	2.2 ± 0.2	9	1.01 ± 0.10	0.136 ± 0.005	1.6 ± 0.2	6
Sub-surface water	51-200	33.09 ± 0.22	3.2 ± 0.5	-0.5 ± 1.2	4.6 ± 0.7	1.3 ± 0.1	56 ± 2	2.0 ± 0.1	5	0.95 ± 0.08	0.141 ± 0.004	1.7 ± 0.2	5
Intermediate water	500*	34.00 ± 0.03	3.7 ± 0.1	-0.2 ± 1.8	1.7 ± 1.4	1.2 ± 0.2	48 ± 2	2.1 ± 0.2	2	0.75 ± 0.12	0.146 ± 0.009	1.6 ± 0.2	2
Deep water	≥1000	34.47 ± 0.16	2.3 ± 0.6	-1.9 ± 0.8	1.7 ± 0.5	1.0 ± 0.1	45 ± 2	1.9 ± 0.2	4	0.74 ± 0.01	0.149 ± 0.004	1.7 ± 0.1	4
Bering Shelf													
Alaskan Coastal	\	30.46 ± 1.37	7.2 ± 2.0	1.2 ± 0.6	10.7 ± 3.9	3.9 ± 1.8	96 ± 22	3.3 ± 0.7	12	2.77 ± 1.15	0.193 ± 0.027	2.6 ± 0.5	5
Water (S ≤ 31.8)													
Bering Shelf Water	\	32.05 ± 0.21	3.6 ± 1.8	1.4 ± 1.0	6.0 ± 0.8	2.0 ± 0.2	71 ± 4	2.4 ± 0.2	9	1.24 ± 0.04	0.166 ± 0.020	1.6 ± 0.1	2
$(31.8 \le S \le 32.5)$													
Chukchi Sea													
Southern surface	0-20	31.29 ± 0.39	6.5 ± 1.1	3.2 ± 1.2	6.7 ± 1.3	2.5 ± 0.4	82 ± 8	2.5 ± 0.3	9	1.46 ± 0.12	0.148 ± 0.010	1.7 ± 0.1	6
water (<71°N)													
Northern surface	0-20	28.75 ± 1.65	0.2 ± 1.3	10.2 ± 5.0	8.3 ± 1.3	2.3 ± 0.2	73 ± 2	2.6 ± 0.2	16	1.30 ± 0.15	0.148 ± 0.008	1.8 ± 0.2	6
water (71-73°N)													
Sub-surface water	>20	32.31 ± 0.21	0.3 ± 2.0	0.4 ± 1.0	6.0 ± 0.9	2.1 ± 0.3	71 ± 3	2.5 ± 0.3	22	1.15 ± 0.13	0.141 ± 0.012	1.6 ± 0.1	11
Canada Basin													
Polar surface water $(S < 32)$	0–75	29.45 ± 1.72	-0.8 ± 0.8	0.8 ± 3.5	14.0 ± 2.7	2.6 ± 0.3	73 ± 3	2.9 ± 0.3	32	1.63 ± 0.17	0.171 ± 0.013	2.2 ± 0.2	18
Upper halocline	75-200	32.75 ± 0.56	-1.3 ± 0.2	-2.2 ± 1.1	7.0 ± 1.9	2.1 ± 0.2	65 ± 2	2.7 ± 0.3	26 [§]	1.21 ± 0.07	0.156 ± 0.005	1.9 ± 0.1	16
water $(32 < S < 34)$	70 200	52.75 ± 6.66	1.5 ± 0.2	2.2 _ 1.1	7.10 ± 7.19	2.1 = 0.2	00 ± 2	2., _ 0.5		1.21 = 0.07	0.100 ± 0.000	117 = 011	10
Lower halocline	200-	34.50 ± 0.23	0 ± 0.5	-1.1 ± 1.1	1.0 ± 1.4	1.6 ± 0.3	59 ± 3	2.2 ± 0.3	13	0.98 ± 0.07	0.153 ± 0.011	1.7 ± 0.1	6
water	300			. —									
(34 < S < 34.8)													
Intermediate water	301-	34.84 ± 0.02	0.5 ± 0.3	-0.4 ± 1.1	-0.7 ± 0.9	1.2 ± 0.2	53 ± 1	1.9 ± 0.3	15	0.93 ± 0.08	0.150 ± 0.007	1.8 ± 0.2	10
	800												
Deep Water	>1000	34.90 ± 0.03	-0.2 ± 0.2	0.3 ± 1.2	-1.4 ± 1.0	1.0 ± 0.2	49 ± 3	1.7 ± 0.3	13	0.87 ± 0.09	0.144 ± 0.009	1.8 ± 0.2	11

^{*} Two samples collected at the depth of 500 m were available for the intermediate water; § There were 25 δ^{18} O data available for UHW and thus, the averages of SIM and meteoric water ware calculated based on these 25 δ^{18} O data.

we encountered previously defined water masses (Jones and Anderson, 1986; Chen et al., 2003; Alkire et al., 2010). The polar surface water, with an average salinity of 29.5 ± 0.7 , resided in the upper 75 m. The upper halocline water lay between 75 m and 200 m with a core salinity of 32.8 ± 0.6 . The lower halocline water, immediately beneath the upper halocline water, had a core salinity of 34.5 ± 0.2 and temperature of 0 ± 0.5 °C (Table 1 and Fig. 4). Water masses encountered below 300 m were: the warm intermediate water $(0.5 \pm 0.3$ °C) from the Atlantic Ocean; and the cold deep Arctic Ocean water (≥ 1000 m, -0.2 ± 0.2 °C) (Table 1).

2.2. Sample collection

Seawater was collected on-board *R/V Xuelong* using Niskin bottles on a CTD-rosette. A total of 187 seawater samples were collected at different depths across 31 stations from the Bering Sea to Canada Basin (Fig. 1). Eleven stations were occupied in the Bering Sea, of which 6 stations were on the Bering Shelf and 5 stations were in the basin and slope areas (called the Bering Basin hereafter). In the Chukchi Sea, there were 10 stations on the shelf with depths less than 100 m. The other 10 stations were distributed in the southern and western Canada Basin (Fig. 1).

Seawater for δ^{18} O analysis was directly collected from Niskin bottles and sealed in polyethylene bottles

(~30 mL). Samples were kept in the dark at room temperature until analysis. Seawater for DBC, CDOM and DOC analysis was filtered on board through pre-combusted (450 °C, 4 h) Whatman GF/F filters. Two aliquots of filtrate (~30 mL each) were transferred into pre-combusted (500 °C for 4 h) brown glass bottles and stored at 4 °C and −18 °C for CDOM and DOC analyses, respectively. Another 2 to 4 liters of filtrate were transferred to a precleaned (rinsed five times with ultrapure water after soaking in 0.1 μmol L⁻¹ HCl for 24 h) polypropylene bottle (Nalgene) and acidified to pH≈2 using 6 mol L⁻¹ HCl for solid phase extraction and eventual DBC measurement. δ^{18} O, CDOM and DOC were determined for all 187 samples. DBC analysis was conducted for 108 samples (Tables 1, A1 and A2).

2.3. DBC analysis

DOC in seawater was extracted using a solid phase cartridge prior to DBC analysis as described in Fang et al. (2017). Briefly, the acidified filtrate was pumped through a solid phase cartridge (500 mg, Hydrophilic-Lipophilic Balance, HLB), followed by another 20 mL of 0.01 μ mol L⁻¹ HCl to remove salts. The cartridge was then dried under a high purity N₂ stream and absorbed DOC was eluted using 6 mL of methanol (High Performance Liquid Chromatography (HPLC) grade, Sigma-Aldrich). The

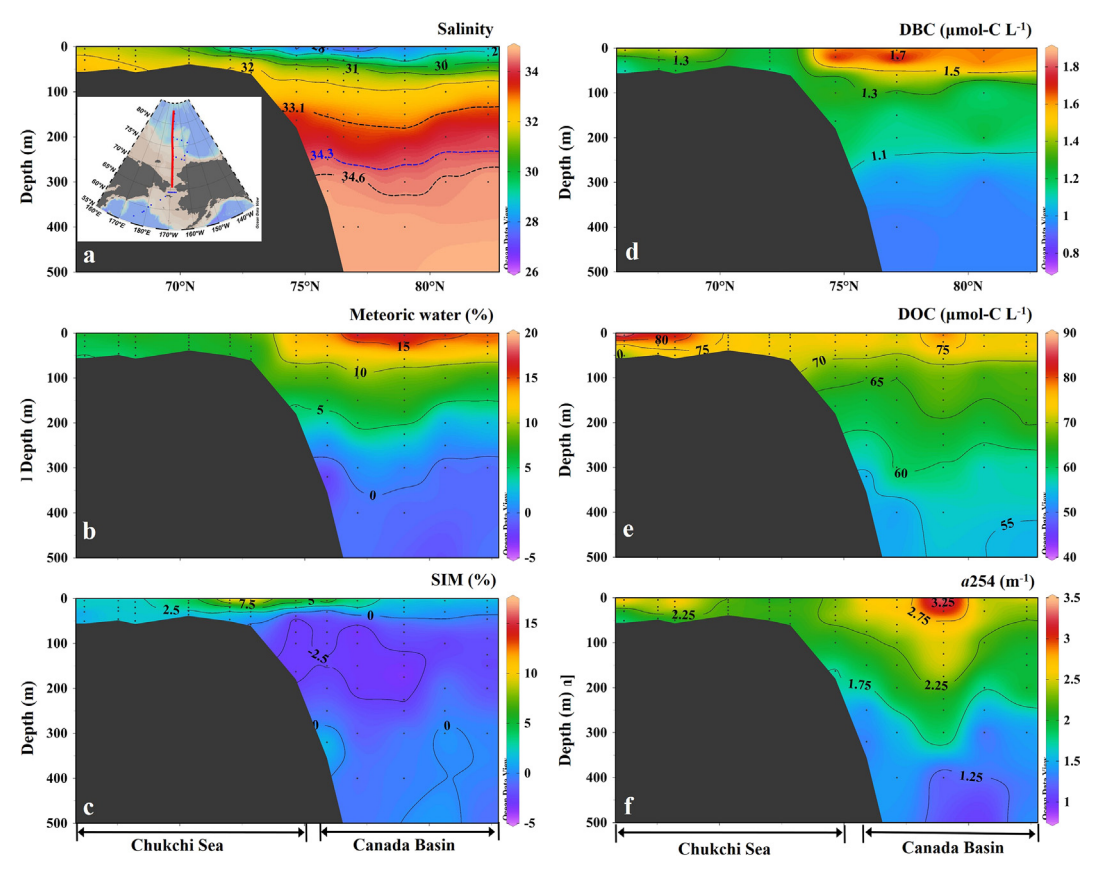


Fig. 4. Vertical distributions of salinity, meteoric water and SIM fractions, and DOMs (i.e., DBC, DOC and CDOM) in the upper water (<500 m) over the Chukchi Sea and Canada Basin.

methanol eluent was stored in a pre-combusted glass bottle at -18 °C until analysis. The average DOC recovery of the solid phase cartridge was $37 \pm 4\%$ for all 108 samples, which was comparable to reported values using PPL (Varian) (Dittmar, 2008) and HP-20 (Sigma Aldrich) (Coppola et al., 2015) columns.

DBC was determined using the benzene polycarboxylic acid (BPCA) method. The principle of BPCA method is that DBC can be oxidized with nitric acid into BPCAs which are then separated and quantified via HPLC (Dittmar, 2008; Wagner et al., 2017). Briefly, about 3 mL of methanol eluent (containing more than 10 μmol-DOC) was dried under a high purity N₂ stream in a pre-combusted (500 °C for 4 h) glass ampoule. About 0.5 mL of 65% HNO₃ was added into the ampoule. The ampoule was then flame sealed and heated at 160 °C for 6 hours in an oven. DBC was converted to BPCAs during oxidation (Dittmar, 2008). Nitric acid in the ampule was dried under argon gas at ~ 50 °C in a sand bath. The residual sample was re-dissolved in 650 μL of mobile phase A (40 mL phosphoric acid (HPLC grade, Fisher Chemical) in 1 L ultrapure water) for further BPCA analysis using an HPLC system equipped with an ultraviolet detector (Shimadzu). BPCAs were separated using an Agilent Poroshell 120 phenyl-hexyl column (4.6 × 150 mm, 2.7 µm) with aqueous gradient of mobile phase A and B (2.42 g NaH₂PO₄·H₂O and 0.64 g Na₂HPO₄·7H₂O (Fisher Chemical) in 1 L ultrapure water; Wagner et al., 2017). The injection volume was 25 µL. Though absorbance signal at 240 nm was previously used during BPCAs quantification (Dittmar, 2008, Stubbins et al., 2012a, 2015), absorbance intensities of the two most important BPCAs. i.e., benzenepentacarboxylic acid (B5CA) and mellitic acid (B6CA), at 205 nm are greater than at 240 nm under the optimized gradient elution. Thus, BPCAs were identified based on their retention times and quantified by the absorbance signal at 205 nm. A standard mixture of six commercial BPCAs (hemimellitic acid, 1,2,3-B3CA; trimellitic acid, 1,2,4-B3CA; trimesic acid, 1,3,5-B3CA; pyromellitic acid, 1,2,4,5-B4CA; B5CA; B6CA) was used to calculate the BPCA concentrations.

The DBC concentration was calculated from the detected BPCA concentrations. Based on a conservative estimate of average carbon atoms within DBC molecules identified by FT-ICR-MS in a variety of natural waters, Dittmar (2008) proposed a formula (i.e., DBC = $33.4 \times (B)$ 6CA] + [B5CA] + 0.5[B4CA] + 0.5[B3CA])) to convert molar BPCA concentrations into DBC concentration (carbon equivalent). Later, some studies (i.e., Stubbins et al., 2012a and our experiments) found that B3CAs and 1,2,4,5-B4CA loss can occur during HNO₃-oxidation, while the recoveries of B6CA and B5CA are near 100%. Thus, Stubbins et al. (2012a, 2015) proposed a formula to estimate the DBC concentration using the two stable BPCAs (i.e., B6CA and B5CA), i.e., [DBC, μ mol-C L⁻¹] = 0.0891 \times ([B6CA, nmol L⁻¹] + [B5CA, nmol L⁻¹])^{0.9175}. This relationship provides a robust estimate of DBC concentrations in coastal seas and open oceans (Stubbins et al., 2012a, 2015). HNO₃-oxidation of DBC may produce a little nitrated BPCA (Ziolkowski et al., 2011). Owing to a lack

of approach for quantification, nitrated BPCA is usually not included. In this study, the updated calculation from Stubbins et al. (2015) was used to quantify DBC concentrations.

2.4. DOC measurement

Seawater samples were acidified to pH 2 by adding phosphoric acid. The DOC concentration was measured using a Shimadzu TOC-VPCH analyzer (Lin et al., 2016). Potassium hydrogen phthalate was used to prepare standard solutions with concentrations ranging from 10 to 200 $\mu mol\text{-}C$ L^{-1} . The deep seawater reference from the Consensus Reference Material Project (CRM, https://hansell-lab.rsmas.miami.edu/consensus-reference-material/index.html) was used to check the accuracy of analysis. The deviation of CRM analysis was less than 5% and the standard errors of DOC concentration were generally less than 4%.

2.5. Absorbance of dissolved organic matter (DOM)

CDOM absorbance was determined on a Shimadzu UV2450 spectrophotometer using a 5 cm quartz cuvette. The absorption spectrum was measured in triplicate from 240 to 800 nm with 0.5 nm intervals. The absorption coefficient at 254 nm (i.e., a254) was used as an indicator of CDOM and calculated as $a254 = \ln(10) \times A_{254}/l$, where A_{254} is the absorbance signal at 254 nm and l is the length of cuvette (Hu et al., 2002; Lin et al., 2016).

2.6. Stable oxygen isotope analysis and meteoric water calculation

In the laboratory, 2 mL of seawater sample was transferred to a 2-mL glass vial and tightly sealed before δ^{18} O measurement. Oxygen isotopic composition in seawater was determined using a laser spectroscopy analyzer (Picarro L2140-I, USA) (Li et al., 2017). The precision of the δ^{18} O values was better than \pm 0.03% and calibrated against Vienna Standard Mean Ocean Water (VSMOW) and Standard Light Antarctic Precipitation (SLAP) from the International Atomic Energy Agency (IAEA). δ^{18} O values are reported in per mil relative to VSMOW (i.e., $\delta^{-18}O = \left[\frac{\left(-^{18}O/^{-16}O\right)_{sample}}{\left(-^{18}O/^{-16}O\right)_{ISMOW}} - 1\right] \times 1000) \text{ (Table A1)}.$

$$\delta^{-18}O = \left[\frac{\left(-^{18}O/ -^{16}O \right)_{sample}}{\left(-^{18}O/ -^{16}O \right)_{ISMOW}} - 1 \right] \times 1000) \text{ (Table A1)}.$$

Hydrographic processes, such as river water input and sea-ice formation/thaw, affect DOC distribution in the Arctic Ocean and its adjacent seas (Hansell et al., 2004; Cooper et al., 2005; Shen et al., 2016). To assess the contribution of SIM and meteoric water in Arctic Ocean waters, a three end-member mass balance model, including Pacific Ocean water (PW), meteoric water and SIM, was established based on salinity and $\delta^{18}O$ (Tong et al., 2014; Pan et al., 2015; Li et al., 2017). The fractions of meteoric water and SIM were estimated using Eqs. (1), (2) and (3):

$$f_{PW} + f_{SIM} + f_{meteor} = 1 \tag{1}$$

$$f_{PW}S_{PW} + f_{SIM}S_{SIM} + f_{meteor}S_{meteor} = S_m$$
 (2)

$$f_{PW}\delta^{18}O_{PW} + f_{SIM}\delta^{18}O_{SIM} + f_{meteor}\delta^{18}O_{meteor} = \delta^{18}O_{m}$$
 (3)

where f, S and δ^{18} O are the fraction, salinity and δ^{18} O of each end-member water mass respectively, and "m" and "meteor" signify the measured values and meteoric water, respectively. The meteoric water end-member δ^{18} O value in Arctic rivers varies with season averaging -22.2% during the spring freshet and -20.9% across the year (Holmes et al., 2020a; Shiklomanov et al., 2020). We assessed the degree to which this variability in the meteoric water endmember δ^{18} O values influenced estimated meteoric water fractions in our samples (Table A3). Results indicated that use of two end-member values resulted in a difference of less than 5% in estimated meteoric water fractions. Thus, for consistency with previous literature, widely used endmember values for salinity and $\delta^{18}O$ (i.e., PW: S = 34.51, $\delta^{18}O = -0.06\%$; SIM: S = 6, $\delta^{18}O = 1.9\%$; meteoric water: S = 0, $\delta^{18}O = -21\%$) were adopted in our study (Östlund and Hut, 1984; Cooper et al., 2005; Pan et al., 2015). The model-derived fractions of meteoric water and SIM are presented in Tables 1 an A1. Negative values of SIM are interpreted as the presence of brine water, which is generated during sea ice formation (Tong et al., 2014; Li et al., 2017). In addition, rainwater cannot be distinguished from river water in meteoric water based on salinity and δ^{18} O data. Carmack et al. (2016) reviewed the contribution of net precipitation to meteoric water from 2000 to 2010 in the Arctic Ocean and estimated that net precipitation comprises ~ 23% of meteoric water. To preliminarily assess the influence of precipitation on DBC in the Arctic Ocean, this information was adopted in our study.

3. RESULTS

3.1. DBC, CDOM and DOC concentrations

On the Bering Shelf, the Alaskan Coastal Water showed the highest DBC (2.8 \pm 1.2 $\mu mol\text{-C}$ L^{-1}), DOC (96 \pm 22 $\mu mol\text{-C}$ L^{-1}) and a254 (3.9 \pm 1.8 m^{-1}). The Bering Shelf Water showed lower DBC (1.24 \pm 0.04 $\mu mol\text{-C}$ L^{-1}), DOC (71 \pm 4 $\mu mol\text{-C}$ L^{-1}) and a254 (2.0 \pm 0.2 m^{-1})

(Table 1 and Fig. 2). The surface water in the Bering Basin exhibited the lowest DBC, DOC concentrations and a254 values, averaging 1.0 \pm 0.1 $\mu mol\text{-C}$ $L^{-1},~64$ \pm 5 $\mu mol\text{-C}$ L^{-1} and 1.7 \pm 0.2 m⁻¹, respectively (Table 1). DBC (1.5 \pm 0.1 μ mol-C L⁻¹) and DOC (82 \pm 8 μ mol-C L⁻¹) in the surface water of the southern Chukchi Sea were higher than those in the northern Chukchi Sea (DBC: $1.3 \pm 0.2 \mu mol$ C L⁻¹; DOC: $73 \pm 2 \mu \text{mol-C L}^{-1}$), while a254 values were comparable across the Chukchi Sea (Table 1 and Fig. 3). In the Canada Basin, high values of DBC, DOC, a254 (DBC: 1.6 ± 0.2 μmol-C L⁻¹; DOC: 73 ± 3 μmol-C L⁻¹; a254: 2. $6 \pm 0.3 \text{ m}^{-1}$) were observed in the polar surface water, followed by the upper halocline water (DBC: 1.2 ± 0.1 µmol-C L⁻¹; DOC: $65 \pm 2 \mu \text{mol-C L}^{-1}$; a254: $2.1 \pm 0.2 \text{ m}^{-1}$). Below the upper halocline water. DBC and a254 were low and showed little variation while DOC decreased slightly with depth (Fig. 5).

3.2. BPCA ratio and SUVA₂₅₄

The ratio of B6CA to B5CA (defined as B6/B5 hereafter) has been used to indicate the aromatic condensation of DBC (Dittmar, 2008). In general, riverine DBC tends to be more condensed (higher B6/B5) than DBC in seawater (lower B6/B5) (Ziolkowski and Druffel, 2010; Coppola et al., 2015; Stubbins et al., 2015). The SUVA₂₅₄, i.e., DOC-normalized a254, is a good indicator of the percentage of DOC that is aromatic (Weishaar et al., 2003). The two proxies, thereby, were employed to examine the impact of river discharge on DBC quality and DOC aromaticity. SUVA₂₅₄ and the B6/B5 ratio showed similar distributions. The surface water in the Bering Basin showed low SUVA₂₅₄ (2.2 \pm 0.2 L mg⁻¹ m⁻¹) and B6/B5 ratio (0.136 \pm 0.005). On the contrary, the Alaskan Coastal Water presented high SUVA₂₅₄ (3.3 \pm 0.7 L mg⁻¹ m⁻¹) and B6/B5 ratio (0.193 \pm 0.027). In the Chukchi Sea, SUVA₂₅₄ (2.6 L mg⁻¹ m⁻¹) and B6/B5 (0.141-0.148) were a little higher than that in the surface water of the Bering Basin but lower than the Alaskan Coastal Water. In the Canada Basin, SUVA₂₅₄ (2.9 \pm 0.3 L mg⁻¹ m⁻¹) and B6/B5

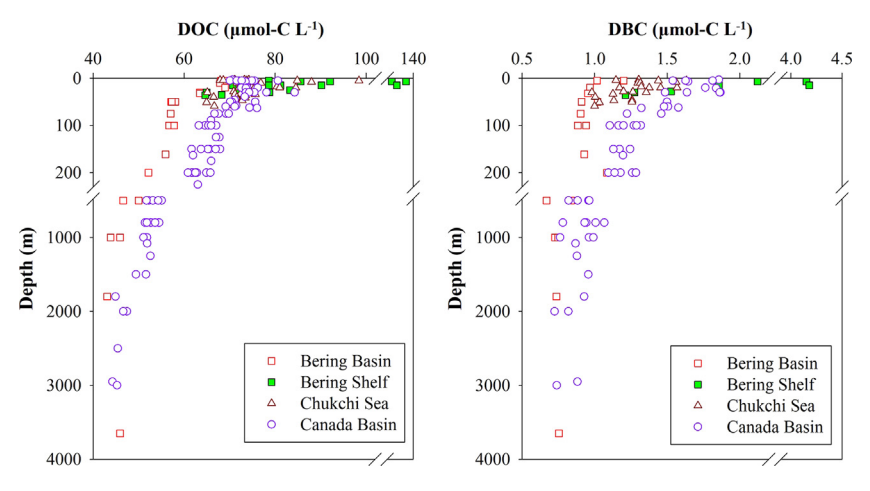


Fig. 5. Depth profiles of the DOC and DBC in the western Arctic Ocean and the Bering Sea.

 (1.63 ± 0.17) were high in the surface water and gradually decreased with depth (Table 1).

4. DISCUSSION

4.1. The role of freshwater in affecting the DBC and DOC patterns

In the northern high-latitude oceans, freshwater from river discharge, precipitation and seasonal sea-ice melting (Proshutinsky et al., 2009; Tong et al., 2014; Alkire et al., 2017), shapes the DOC distribution and water stratification (Mathis et al., 2005; Shen et al., 2016). In this study, the DBC and δ^{18} O data allowed us to examine the influence of different freshwater sources on the spatial characteristic of DBC. Inclusion of DOC and *a*254 analyses allowed examination of the geochemical behaviors of DBC, DOC and CDOM.

4.1.1. The Bering Sea

DBC concentrations were higher in the shelf water, especially the Alaskan Coastal Water, than in the upper water of the Bering Basin. Also, the shelf water showed higher B6/B5 values (Table 1). Since river water DBC usually has higher B6/B5 values than seawater DBC (Ziolkowshi and Druffel, 2010; Stubbins et al., 2015), these results indicated the significant impact of riverine discharge on the DBC distribution in the Bering Shelf. Higher values for DOC concentration, a254 and SUVA₂₅₄ indicate that DOC in shelf waters is more terrigenous than the DOC in the Bering Basin (Table 1 and Fig. 2). Rivers discharge more than 300 km³ yr⁻¹ of freshwater to the Bering Shelf, of which ~ 200 km³ yr⁻¹ comes from the Yukon River, and ~ 75 km³ yr⁻¹ from the Kuskokwim, Nushagak, and Kvichakand Rivers (Aagaard et al., 2006; Amon et al., 2012; Alkire et al., 2017). The most intense periods of discharge usually occur during the boreal spring/early summer (Holmes et al., 2020b). This river water carries riverine DBC and DOC to the shelf area (Holmes et al., 2008; Stubbins et al., 2015).

DBC, *a*254 and DOC were correlated with meteoric water fractions (Fig. S2) in the Bering Shelf, suggesting rivers could be a major source of DOC and DBC. Precipitation also adds meteoric water to the surface ocean. However, DBC, DOC and CDOM all occur at low concentrations in Arctic precipitation (DBC: 0.13 μmol-C L⁻¹, Khan et al., 2017; DOC: 16 μmol-C L⁻¹, Zhang et al., 2020; *a*254: 0.19 m⁻¹, Stubbins et al., 2012b). Thus, inputs of riverine DBC and DOC were the likely driver of the positive correlations between meteoric water, DBC, DOC and *a*254 in the Bering Shelf (Fig. S2).

In the upper Bering Basin, lower DBC, CDOM and DOC concentrations and meteoric water fraction relative to the shelf region suggested less impact of river runoff on DOM. It can be attributed to the strong northwest flow of the Bering Slope Current (Fig. 1), preventing the intrusion of the Bering Shelf water from getting into the Bering Basin (Coachman, 1986; Li et al., 2017). Thus, during the summer, the spatial pattern of DBC, DOC and CDOM in the Bering Sea appeared to be largely

regulated by the river discharge and the local current system.

4.1.2. The Chukchi Sea

Unlike the Bering Sea, DBC concentration, as well as DOC and a254 signals, did not show high values in samples with low salinity in the Chukchi Sea (Fig. 6), indicating that river water is not the dominant factor in controlling the spatial pattern of DBC or freshwater. In fact, the SIM comprised large portions of freshwater in the surface water of northern Chukchi Sea (Table 1), which is located in the front of ice margin zone during the cruise. Interestingly, both the DBC and DOC concentrations decreased with increasing SIM in sea ice impacted samples (i.e. samples with SIM > 3.5%; Fig. 7), revealing a dilution effect of SIM on DBC and DOC. DOC concentration in the Arctic sea-ice has an average of \leq 55 µmol-C L⁻¹ (Zabłocka et al., 2020), which is much lower than the DOC concentration of Arctic river water (Stubbins et al., 2015). The concentration of DBC has not been reported for sea ice, though its presence in the sea ice has been identified by Fourier transform ion cyclotron resonance mass spectrometry (Longnecker, 2015; Brogi et al., 2018). However, the decrease in DBC concentration with increasing SIM contributions to samples (Fig. 7) suggested that SIM is likely depleted in DBC relative to river water and seawater. For samples less impacted by SIM (SIM < 3.5%), DBC and DOC concentrations increased with decreasing salinity (Fig. 6d and 6f), similar to patterns observed in the Bering Shelf. These results suggest that SIM drove the negative trend in DBC vs. salinity in the Chukchi Sea.

4.1.3. The Canada Basin

DBC concentration showed similar spatial patterns to meteoric water in the surface water of the Canada Basin (Fig. 4). Further, all DBC, *a*254 and DOC signals decreased with increasing salinity in the upper layer of the Canada Basin (≤200 m) (Fig. 6), implying that riverine input controlled the spatial distributions of DBC and DOC in the surface water during the summer. Previous studies confirm the entrapment of the Pan-Arctic river water in the upper Canada Basin due to the convergence of the Beaufort Gyre (Guay et al., 2009; Proshutinsky et al., 2009; Morison et al., 2012; Pickart et al., 2013). Hence, the Canada Basin appears to be an important reservoir of riverine DBC.

Below 200 m, the intermediate and deep water showed much lower DBC concentrations than the upper ocean (Fig. 5). In addition, both B6/B5 and SUVA₂₅₄ exhibited decreasing values with depth (Table 1). These results consistently indicated that the influence of river water on DBC and DOC weakened in the intermediate and deep water. In the deep water of the Canada Basin, the DBC concentrations ranged from 0.72 to 0.99 µmol-C L⁻¹ (Fig. 5), comparable to the averages of 0.74 ± 0.01 µmol-C L⁻¹ (n = 4) in the Bering Basin, the range of 0.60-0.80 µmol-C L⁻¹ in the Southern Ocean (Dittmar and Paeng, 2009), and the average of 1.06 ± 0.16 µmol-C L⁻¹ in the Atlantic Ocean (Stubbins et al., 2012a). These results suggest that the refractory nature of DBC in aphotic waters enables DBC to disperse homogenously in global deep oceans. Thus,

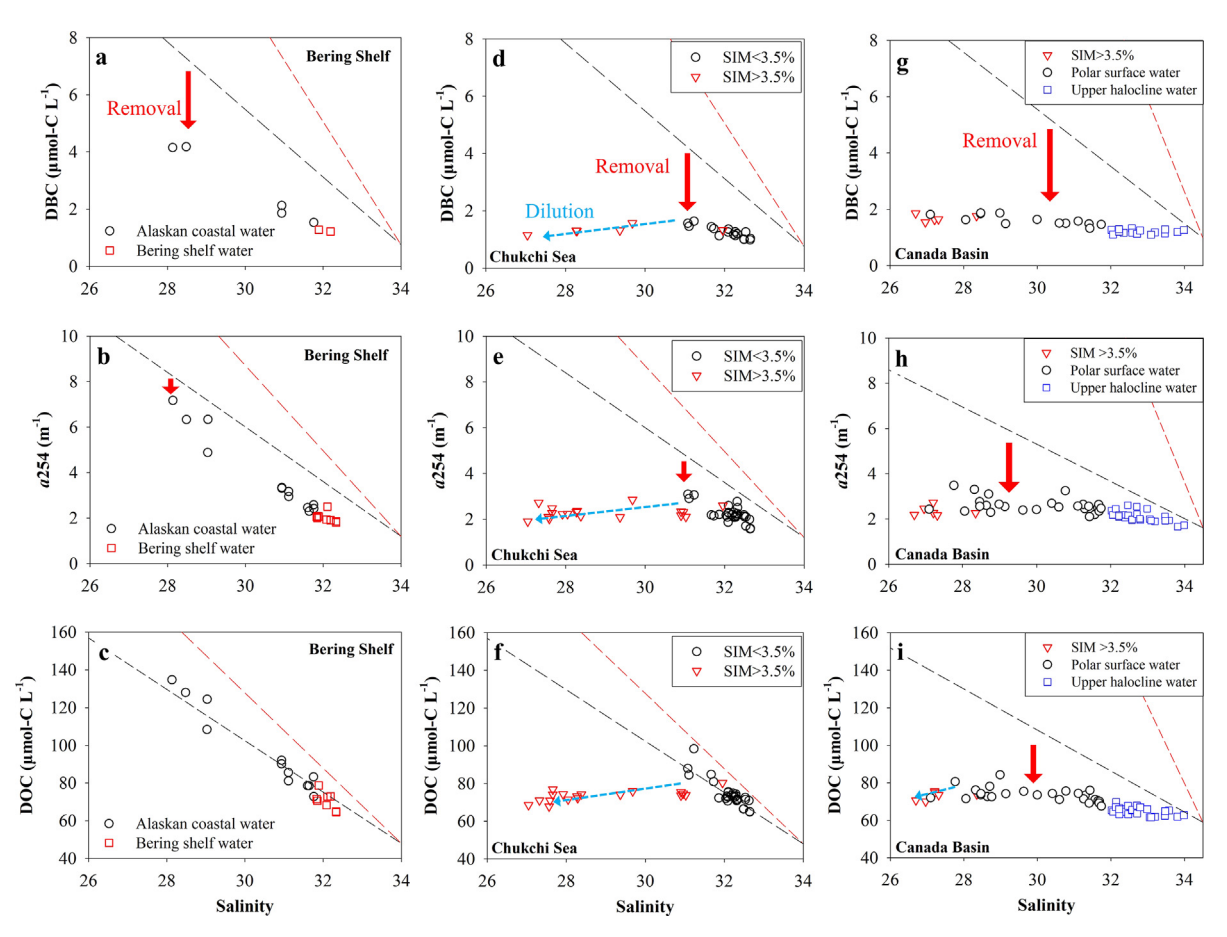


Fig. 6. Distributions of DOMs (i.e., DOC, CDOM and DBC) along with salinity in study regions. Black and red dash lines represent lowerand upper-limit of the conservative mixing between riverine and oceanic end-members.

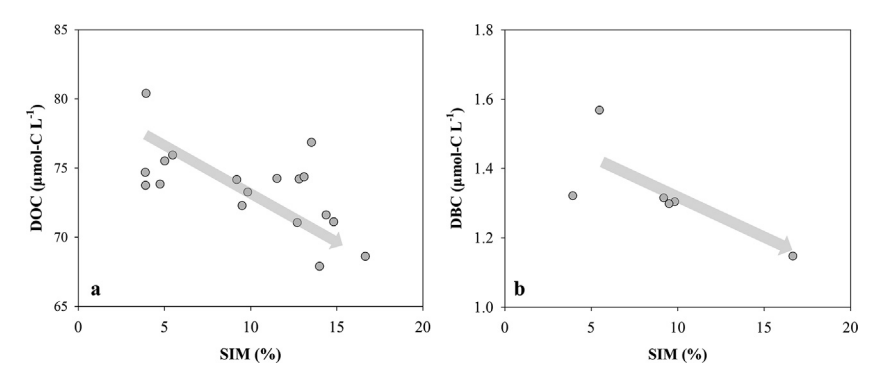


Fig. 7. Variations of DBC and DOC with SIM content (SIM > 3.5%) in the Chukchi Sea.

DBC in deep water might show conservative behavior as supported by its relationship with salinity in the mesopelagic water of the South China Sea (Fang et al., 2017).

4.2. Removal of DBC in the western Arctic Ocean

As discussed above, riverine input plays a key role in the DBC distribution over the Bering Shelf and western Arctic Ocean during the boreal summer. Arctic rivers discharge 2.8 ± 0.3 Tg yr⁻¹ of DBC to the ocean (Stubbins et al.,

2015). However, the fate of riverine DBC in coastal seas and the Arctic Ocean is still poorly understood. In order to examine the removal of DBC, we compared *in situ* DBC concentrations with the conservative mixing lines connecting the river to the ocean end-member in each specific region (i.e., the Bering Shelf, Chukchi Sea, and Canada Basin) (Fig. 6). The end-member values for the conservative mixing lines are provided in Table 2 and supplementary materials. We plotted two conservative mixing lines, representing the upper- and lower- limits of river end-member

Table 2 Salinity, DOC, *a*254 and DBC values of river water and seawater end-members. End-member values are estimated based on data from 1. Holmes et al. (2020a, 2020b); 2. Shiklomanov et al. (2020); 3. Stubbins et al. (2015); 4. This study.

Parameters	Bering Shelf	Chukchi Shelf	Canada Basin
River water end-member			
Salinity	0	0	0
DOC concentration (μmol-C L ⁻¹) ^{1,2}	511–726	511–726	436-1483
$a254 \text{ (m}^{-1})^{1,2}$	42–65	42–65	30-140
DBC concentration (µmol-C L ⁻¹) ³	41–74	41–74	36–114
Seawater end-member			
Salinity ⁴	34.0	34.0	34.5
DOC concentration (μmol-C L ⁻¹) ⁴	48	48	59
$a254 \text{ (m}^{-1})^4$	1.2	1.2	1.6
DBC concentration (μmol-C L ⁻¹) ⁴	0.75	0.75	0.98

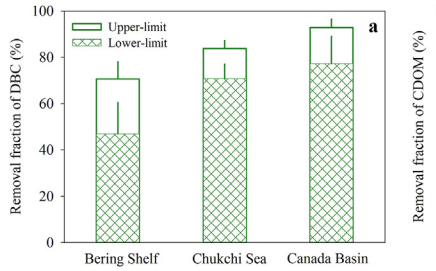
values due to the seasonal variation of DBC concentrations in the Arctic rivers (Table A4). Overall, measured DBC data fell below the two conservative limit mixing lines, suggesting removal of DBC after export to the oceans. Using the same approach also suggested the removal of DOC and CDOM in the shelf and basin regions (Fig. 6), agreeing with previous reports (Hansell et al., 2004; Alling et al., 2010, 2012; Stedmon et al., 2011).

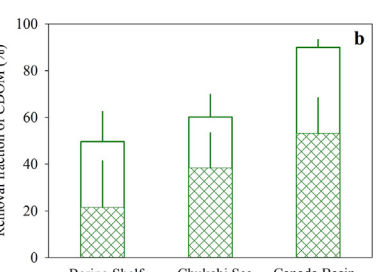
The removal fraction of riverine DBC can be quantified based on the negative departures of DBC from the mixing lines. A few caveats influencing the estimation of DBC removal in this way must be noted: (1) Sea-ice melting affects the evaluation through dilution of DBC, while adding freshwater (Fig. 7). In an attempt to eliminate the influence of sea-ice melting, samples with SIM > 3.5% were excluded; (2) Net precipitation, comprising ~ 23% of the meteoric water in the Arctic Ocean (Carmack et al., 2016), should also be considered in the estimation of DBC removal. Based on available data, the average DOC and DBC concentrations and a254 value of the Arctic precipitation are 16 µmol-C L⁻¹ (Zhang et al., 2020), $0.13 \mu \text{mol-C L}^{-1}$ (Khan et al., 2017) and 0.19 m⁻¹ (Stubbins et al., 2012b), respectively (Table A4). Thus, these values were assigned to the precipitation. The removal of riverine DBC in each region were then plotted in Fig. 8.

On the Bering Shelf, an estimated 47%-71% of riverine DBC was removed (Fig. 8). The removal increased to 71%-84% in the Chukchi Sea and 77%-93% in the upper Canada Basin (Fig. 8). Overall, the majority of riverine DBC was removed within the shelf regions and less than

23% was transported into the Canada Basin (Fig. 8). This result indicated that Arctic shelf regions are likely important sink sites for riverine DBC during the summer. This result may be broadly applicable to other shelf regions. Thus, efficient removal in shelf systems may explain why there is little signature of riverine DBC in the open Atlantic and Pacific Oceans (Wagner et al., 2019). Sinks on the shelf could be due to photo-degradation (Stubbins et al., 2012a) or absorption to sinking particles (Coppola et al., 2014).

The removal of riverine DOC and CDOM was also estimated using the same method as for DBC. Losses of DOC and CDOM were much lower than for DBC (Fig. 8). It has been demonstrated that bulk DOC is less sensitive to photo-degradation than DBC (Stubbins et al., 2012a). In addition, due to the hydrophobic groups contained in DBC, DBC may more readily absorb onto sinking particles than bulk DOC or CDOM. Since our samples were collected during the summer, the elevated solar radiation and primary productivity would enhance the removal of DBC via either photo-degradation or particle absorption on the shelves, resulting in more intense removal of DBC than bulk DOC. Yet, there are some caveats to consider. Estimates of riverine DOC and CDOM removal are likely underestimated due to the production of autochthonous, marine DOC (Mathis et al., 2007; Brogi et al., 2018) and CDOM (Stedmon and Nelson, 2014). In the ice-free region of the Chukchi Sea, for example, surface water holds higher DOC but similar SUVA₂₅₄ compared to the sub-surface water (Table 1), indicating the elevated DOC in the surface water is partly derived from in situ primary productivity rather than river discharge.





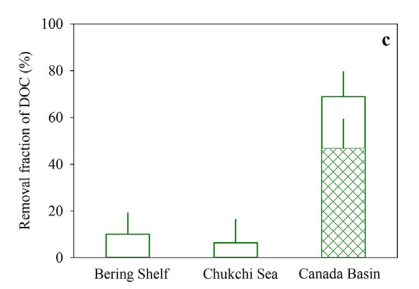


Fig. 8. Removal fraction of DBC, DOC and CDOM derived from their departures from the conservative mixing lines (Fig. 6).

In boreal summer, primary production supplies up to $14 \, \mu mol\text{-C} \, L^{-1}$ of autochthonous DOC to the surface water (Mathis et al., 2007), which would lead to an underestimation of riverine DOC and CDOM removal. In contrast, primary production does not add DBC to the water column and has no influence on the estimation of DBC removal. Thus, both the production of autochthonous DOC and slow removal collectively resulted in the lower apparent losses of riverine DOC than DBC.

The observed DBC characteristics were closely related to the melting of sea ice, river water flushing, and seasonal highs in solar insolation in summer. These and other conditions change seasonally; consequently, the behavior of DBC in seawater observed during this study may not extend to other time periods.

5. CONCLUSION

Our study provided a first look into the distribution and removal of DBC in the western Arctic Ocean during the boreal summer. Freshwater showed contrasting influences on the DBC distribution. River water was the predominant source of DBC to the Bering Shelf and western Arctic Ocean. In sea-ice melt free (SIM < 3.5%) surface water, DBC decreased with increasing salinity, suggesting that DBC-enriched river water determined the spatial pattern of DBC during the summer. By contrast, in SIM impacted waters (SIM > 3.5%), SIM added freshwater, but diluted DBC and DOC.

The measured DBC, DOC and a254 deviated from conservative mixing lines, suggesting their removal during transport from the river to the open ocean. We estimate that 47-84% of riverine DBC was removed within the shelf regions (i.e., Chukchi Sea and Bering Shelf), and < 23% of riverine DBC was transported to the upper Canada Basin. Thus, the shelf regions appear to play an important role in determining the amount of riverine DBC reaching the open oceans. The difference in the removal magnitude between riverine DBC, DOC and CDOM likely resulted from the preferential removal of DBC and/or in situ production of DOC and CDOM in the shelf regions during the summer. Our study only presented a snapshot of the summertime DBC characteristic in the western Arctic Ocean. Considering the significant seasonal variations in river discharge and sea-ice, the DBC characteristics in other seasons are required to better understand the cycling of DBC in the Arctic Ocean.

CREDIT AUTHORSHIP CONTRIBUTION STATEMENT

Ziming Fang: Investigation, Formal analysis, Writing original draft. Weifeng Yang: Conceptualization, Investigation, Writing - review & editing. Aron Stubbins: Investigation, Writing - review & editing. Min Chen: Conceptualization, Investigation. Junjie Li: Methodology, Formal analysis. Renming Jia: Methodology, Formal analysis. Qi Li: Methodology, Formal analysis. Jing Zhu: Methodology. Bo Wang: Methodology.

Declaration of Competing Interest

The authors declare that they have no known competing financial interests or personal relationships that could have appeared to influence the work reported in this paper.

ACKNOWLEDGEMENTS

We appreciate the reviewers and editors for their constructive suggestions for improving the presentation of our results. We also thank the crew of the *RIV Xuelong* for their assistance during the cruise. This study was supported by NSFC (42076030 & 41476061 to W. Y. and 41721005 to M. C.) and NSF (OCE1756812 to A.S.). Sasha Wagner, Lixin Zhu and Jay Brandes assisted with DBC analyses. The data supporting the analysis and conclusions can be found in Tables 1, 2, A1, A2, A3 and A4.

APPENDIX A. SUPPLEMENTARY MATERIAL

Supplementary data to this article can be found online at https://doi.org/10.1016/j.gca.2021.04.024.

REFERENCES

- Aagaard K., Weingartner T. J., Danielson S. L., Woodgate R. A., Johnson G. C. and Whitledge T. E. (2006) Some controls on flow and salinity in Bering Strait. *Geophys. Res. Lett.* 33, L19602.
- Alkire M. B., Falkner K. K., Morison J., Collier R. W., Guay C. K., Desiderio R. A., Rigor I. G. and McPhee M. (2010) Sensorbased profiles of the NO parameter in the central Arctic and southern Canada Basin: New insights regarding the cold halocline. *Deep Sea Res. Part I* 57(11), 1432–1443.
- Alkire M. B., Morison J., Schweiger A., Zhang J., Steele M., Peralta-Ferriz C. and Dickinson S. (2017) A meteoric water budget for the Arctic Ocean. J. Geophys. Res. Oceans 122(12), 10020–10041.
- Alling V., Porcelli D., Mörth C.-M., Anderson L. G., Sanchez-Garcia L., Gustafsson Ö., Andersson P. S. and Humborg C. (2012) Degradation of terrestrial organic carbon, primary production and out-gassing of CO₂ in the Laptev and East Siberian Seas as inferred from δ¹³C values of DIC. Geochim. Cosmochim. Acta 95, 143–159.
- Alling V., Sanchez-Garcia L., Porcelli D., Pugach S., Vonk J. E., van Dongen B., Mörth C.-M., Anderson L. G., Sokolov A., Andersson P., Humborg C., Semiletov I. and Gustafsson Ö. (2010) Nonconservative behavior of dissolved organic carbon across the Laptev and East Siberian seas. *Global Biogeochem. Cy.* 24(4) GB4033.
- Amon R. M. W., Rinehart A. J., Duan S., Louchouarn P., Prokushkin A., Guggenberger G., Bauch D., Stedmon C., Raymond P. A., Holmes R. M., McClelland J. W., Peterson B. J., Walker S. A. and Zhulidov A. V. (2012) Dissolved organic matter sources in large Arctic Rivers. *Geochim. Cosmochim. Acta* 94, 217–237.
- Brogi S. R., Ha S.-Y., Kim K., Derrien M., Lee Y. K. and Hur J. (2018) Optical and molecular characterization of dissolved organic matter (DOM) in the Arctic ice core and the underlying seawater (Cambridge Bay, Canada): Implication for increased autochthonous DOM during ice melting. Sci. Total Environ. 627, 802–811.
- Carmack E. C., Yamamoto-Kawai M., Haine T. W. N., Bacon S., Bluhm B. A., Lique C., Melling H., Polyakov I. V., Straneo F.,

- Timmermans M.-L. and Williams W. J. (2016) Freshwater and its role in the Arctic Marine System: Sources, disposition, storage, export, and physical and biogeochemical consequences in the Arctic and global oceans. J. Geophys. Res. Biogeo. 121, 675-717.
- Chen M., Huang Y., Cai P. and Guo L. (2003) Particulate organic carbon export fluxes in the Canada Basin and Bering Sea as derived from ²³⁴Th/²³⁸U disequilibria. *Arctic* **56**(1), 32–44.
- Coachman L. K. (1986) Circulation, water masses, and fluxes on the southeastern Bering Sea shelf. Cont. Shelf Res. 5(1-2), 23– 108
- Coachman L. K. and Aagaard K. (1974) Physical Oceanography of Arctic and Subarctic Seas. In *Marine Geology and Oceanography of the Arctic Seas* (ed. Y. Herman). Springer, Berlin Heidelberg, pp. 1–72.
- Coachman L. K., Aagaard K. and Tripp R. B. (1975) *Bering Strait: The Regional Physical Oceanography*. University of Washington Press, Seattle and London.
- Cooper L. W., Benner R., McClelland J. W., Peterson B. J., Holmes R. M., Raymond P. A., Hansell D. A., Grebmeier J. M. and Codispoti L. A. (2005) Linkages among runoff, dissolved organic carbon, and the stable oxygen isotope composition of seawater and other water mass indicators in the Arctic Ocean. *J. Geophys. Res. Biogeo.* 110(G2), 308–324.
- Coppola A. I. and Druffel E. R. M. (2016) Cycling of black carbon in the ocean. *Geophys. Res. Lett.* **43**(9), 4477–4482.
- Coppola A. I., Walker B. D. and Druffel E. R. M. (2015) Solid phase extraction method for the study of black carbon cycling in dissolved organic carbon using radiocarbon. *Mar. Chem.* **177** (5), 607–705.
- Coppola A. I., Ziolkowski L. A., Masiello C. A. and Druffel E. R. M. (2014) Aged black carbon in marine sediments and sinking particles. *Geophys. Res. Lett.* 41(7), 2427–2433.
- Dittmar T. (2008) The molecular level determination of black carbon in marine dissolved organic matter. *Org. Geochem.* 39 (4), 396–407.
- Dittmar T. and Paeng J. (2009) A heat-induced molecular signature in marine dissolved organic matter. Nat. Geosci. 2(3), 175–179.
- Dittmar T. and Stubbins A. (2014). Dissolved organic matter in aquatic systems. In: Birrer, B., Falkowski, P., Freeman, K., eds. Treatise on Geochemistry. Elsevier Ltd.
- Fang Z., Yang W., Chen M. and Ma H. (2017) Source and fate of dissolved black carbon in the western South China Sea during the southwest monsoon prevailing season. *J. Geophys. Res. Biogeo.* 122(11), 2817–2830.
- Fang Z., Yang W., Chen M., Zheng M. and Hu W. (2016) Abundance and sinking of particulate black carbon in the western Arctic and Subarctic Oceans. *Sci. Rep.* **6**, 29959.
- Goldberg E. D. (1985) Black Carbon in the Environment. John Wiley, New York.
- Guay C. K. H., McLaughlin F. A. and Yamamoto-Kawai M. (2009) Differentiating fluvial components of upper Canada Basin waters on the basis of measurements of dissolved barium combined with other physical and chemical tracers. *J. Geophys. Res. Oceans* 114, C00A09.
- Hansell D. A., Kadko D. and Bates N. R. (2004) Degradation of terrigenous dissolved organic carbon in the western Arctic Ocean. *Science* 304(5672), 858–861.
- Holmes R. M., McClelland J. W., Raymond P. A., Frazer B. B., Peterson B. J. and Stieglitz M. (2008) Lability of DOC transported by Alaskan rivers to the Arctic Ocean. *Geophys. Res. Lett.* 35, L03402.
- Holmes R. M., McClelland J. W., Tank S. E., Spencer R. G. M. and Shiklomanov A. I. (2020a) Arctic Great Rivers Observatory. Water Quality Dataset, Version 20201030. https://www.arcticgreatrivers.org/data.

- Holmes R. M., McClelland J. W., Tank S. E., Spencer R. G. M. and Shiklomanov A. I. (2020b) Arctic Great Rivers Observatory. Absorbance Dataset, Version 20201030. https://www.arcticrivers.org/data.
- Hu C., Muller-Karger F. E. and Zepp R. G. (2002) Absorbance, absorption coefficient, and apparent quantum yield: A comment on common ambiguity in the use of these optical concepts. *Limnol. Oceanogr.* 47(4), 1261–1267.
- Jaffé R., Ding Y., Niggemann J., Vähätalo A. V., Stubbins A., Spencer R. G. M., Campbell J. and Dittmar T. (2013) Global charcoal mobilization from soils via dissolution and riverine transport to the oceans. *Science* 340(6130), 345–347.
- Jones E. P. and Anderson L. G. (1986) On the origin of the chemical properties of the Arctic Ocean halocline. *J. Geophys. Res. Oceans* 91(C9), 10759–10767.
- Jones M. W., Coppola A. I., Santín C., Dittmar T., Jaffé R., Doerr S. H. and Quine T. A. (2020) Fires prime terrestrial organic carbon for riverine export to the global oceans. *Nat. Commun.* 11, 2791.
- Khan A. L., Wagner S., Jaffe R., Xian P., Williams M., Armstrong R. and McKnight D. (2017) Dissolved black carbon in the global cryosphere: Concentrations and chemical signatures. *Geophys. Res. Lett.* **44**(12), 6226–6234.
- Letscher R. T., Hansell D. A. and Kadko D. (2011) Rapid removal of terrigenous dissolved organic carbon over the Eurasian shelves of the Arctic Ocean. *Mar. Chem.* 123(1-4), 78-87.
- Li Q., Chen M., Jia R., Zeng J., Lin H., Zheng M. and Qiu Y. (2017) Transit time of river water in the Bering and Chukchi Seas estimated from $\delta^{18}O$ and radium isotopes. *Prog. Oceanogr.* **158**, 115–129.
- Lin H., Chen M., Zeng J., Li Q., Jia R., Sun X., Zheng M. and Qiu Y. (2016) Size characteristics of chromophoric dissolved organic matter in the Chukchi Sea. *J. Geophys. Res. Oceans* **121**(8), 6403–6417.
- Longnecker K. (2015) Dissolved organic matter in newly formed sea ice and surface water. Geochim. Cosmochim. Acta 171, 39–49.
- Mathis J. T., Hansell D. A. and Bates N. R. (2005) Strong hydrographic controls on spatial and seasonal variability of dissolved organic carbon in the Chukchi Sea. *Deep Sea Res. Part II* 52(24–26), 3245–3258.
- Mathis J. T., Hansell D. A., Kadko D., Bates N. R. and Cooper L. W. (2007) Determining net dissolved organic carbon production in the hydrographically complex western Arctic Ocean. *Limnol. Oceanogr.* 52(5), 1789–1799.
- Mori T., Kondo Y., Ohata S., Zhao Y., Sinha P. R., Oshima N., Matsui H., Moteki N. and Koike M. (2020) Seasonal variation of wet deposition of black carbon in Arctic Alaska. J. Geophys. Res. Atmos. 125, e2019JD032240.
- Morison J., Kwok R., Peralta-Ferriz C., Alkire M., Rigor I., Andersen R. and Steele M. (2012) Changing Arctic Ocean freshwater pathways. *Nature* **481**(7379), 66–70.
- Nakane M., Ajioka T. and Yamashita Y. (2017) Distribution and Sources of Dissolved Black Carbon in Surface Waters of the Chukchi Sea, Bering Sea, and the North Pacific Ocean. Front. Earth Sci. 5, 34.
- Opsahl S., Benner R. and Amon R. M. W. (1999) Major flux of terrigenous dissolved organic matter through the Arctic Ocean. *Limnol. Oceanogr.* **44**(8), 2017–2023.
- Östlund H. G. and Hut G. (1984) Arctic Ocean water mass balance from isotope data. *J. Geophys. Res. Oceans* **89**(C4), 6373–6381.
- Pan H., Chen M., Tong J., Qiu Y. and Zheng M. (2015) Spatial and temporal variations of freshwater components at a transect near the Bering Strait during 2003-2012. Acta Oceanol. Sin. 37 (11), 135-146. (in Chinese with English abstract)

- Pickart R. S., Spall M. A. and Mathis J. T. (2013) Dynamics of upwelling in the Alaskan Beaufort Sea and associated shelf– basin fluxes. *Deep Sea Res. Part* 176, 35–51.
- Proshutinsky A., Krishfield R., Timmermans M.-L., Toole J., Carmack E., McLaughlin F., Williams W. J., Zimmermann S., Itoh M. and Shimada K. (2009) Beaufort Gyre freshwater reservoir: State and variability from observations. *J. Geophys. Res. Oceans* 114, C00A10.
- Shen Y., Benner R., Robbins L. L. and Wynn J. G. (2016) Sources, distributions and dynamics of dissolved organic matter in the Cannada and Makarov basins. Front. Mar. Sci. 3, 198.
- Shiklomanov A. I., Holmes R. M., McClelland J. W., Tank S. E. and Spencer R. G. M. (2020) Arctic Great Rivers Observatory. Discharge Dataset, Version 20201030. https://www.arcticrivers.org/data.
- Stedmon C. A. and Nelson N. B. (2014) The optical properties of DOM in the ocean. In *Biogeochemistry of Marine Dissolved Organic Matter* (eds. D. A. Hansell and C. A. Carlson), 2nd edition. Academic Press, Elservier, pp. 481–508.
- Stedmon C. A., Amon R. M. W., Rinehart A. J. and Walker R. A. (2011) The supply and characteristics of colored dissolved organic matter (CDOM) in the Arctic Ocean: Pan Arctic trends and differences. *Mar. Chem.* 124(1–4), 108–118.
- Stubbins A., Niggemann J. and Dittmar T. (2012a) Photo-lability of deep ocean dissolved black carbon. *Biogeosciences* **9**(5), 1661–1670.
- Stubbins A., Hood E., Raymond P. A., Aiken G. R., Sleighter R. L., Hernes P. J., Butman D., Hatcher P. G., Striegl R. G., Schuster P., Abdulla H. A. N., Vermilyea A. W., Scott D. T. and Spencer R. G. M. (2012b) Anthropogenic aerosols as a source of ancient dissolved organic matter in glaciers. *Nat. Geosci.* 5(3), 198–201.
- Stubbins A., Spencer R. G. M., Mann P. J., Holmes R. M., McClelland J. W., Niggemann J. and Dittmar T. (2015) Utilizing colored dissolved organic matter to derive dissolved black carbon export by arctic rivers. *Front. Earth Sci.* **3**, 63.
- Tong J., Chen M., Qiu Y., Li Y. and Cao J. (2014) Contrasting patterns of river runoff and sea-ice melted water in the Canada Basin. *Acta Oceanol. Sin.* 33(6), 46–52.

- Wagner S., Brandes J., Goranov A. I., Drake T. W., Spencer R. G. M. and Stubbins A. (2017) Online quantification and compound-specific stable isotopic analysis of black carbon in environmental matrices via liquid chromatography-isotope ratio mass spectrometry. *Limnol. Oceanogr. Meth.* 15(12), 995–1006.
- Wagner S., Brandes J., Spencer R. G. M., Ma K., Rosengard S. Z., Moura J. M. S. and Stubbins A. (2019) Isotopic composition of oceanic dissolved black carbon reveals non-riverine source. *Nat. Commun.* 10, 5064.
- Wagner S., Jaffé R. and Stubbins A. (2018) Dissolved black carbon in aquatic ecosystems. *Limol. Oceanogr. Lett.* **3**(3), 168–185.
- Weishaar J. L., Aiken G. R., Bergamaschi B. A., Farm M. S., Fujii R. and Mopper K. (2003) Evaluation of specific ultraviolet absorbance as an indicator of the chemical composition and reactivity of dissolved organic carbon. *Environ. Sci. Technol.* 37 (20), 4702–4708.
- Zabłocka M., Kowalczuk P., Meler J., Peeken I., Dragańska-Deja K. and Winogradow A. (2020) Compositional differences of fluorescent dissolved organic matter in Arctic Ocean spring sea ice and surface waters north of Svalbard. *Mar. Chem.* 227, 103893
- Zhang Y., Kang S., Gao T., Sprenger M., Dou T., Han W., Zhang Q., Sun S., Du W., Chen P., Guo J., Cui X. and Sillanpää M. (2020) Dissolved organic carbon in Alaskan Arctic snow: concentrations, light-absorption properties, and bioavailability. *Tellus B: Chem. Phys. Meteorol.* 72(1), 1–19.
- Zhao J., Shi J., Gao G., Jiao Y. and Zhang H. (2006) Water mass of the northward throughflow in the Bering Strait in the summer of 2003. *Acta Oceanol. Sin.* **25**(2), 25–32.
- Ziolkowski L. A. and Druffel E. R. M. (2010) Aged black carbon identified in marine dissolved organic carbon. *Geophys. Res. Lett.* **37**(16) L16601.
- Ziolkowski L.A., Chamberlin A. R., Greaves J., and Druffel E. R. M. (2011) Quantification of black carbon in marine systems using the benzene polycarboxylic acid method: a mechanistic and yield study. Limnol. Oceanogr. Meth. 9, 140–149

Associate editor: Elizabeth Ann Canuel